Beat Noise Mitigation of Spectral Amplitude Coding OCDMA Using Heterodyne Detection

Manabu Yoshino, Shin Kaneko, Tomohiro Taniguchi, Noriki Miki, *Member, IEEE*, Kiyomi Kumozaki, *Member, IEEE*, Takamasa Imai, Naoto Yoshimoto, *Member, IEEE*, and Makoto Tsubokawa

***Abstract*—In order to relax the limitation of the number of multiplexed signal lights caused by beat noise between signal lights, we investigate the applicability of a heterodyne detection technique to a spectral amplitude coding optical code division multiple access scheme. In this investigation, for the first time, we found analytically that the optical frequency chips that form parts of the signal and local lights require uniform phase differences even for envelope detection. We also confirm this requirement and our theoretical analysis experimentally.**

***Index Terms*—Code division multiplexing, heterodyne detection, optical fiber communication.**

I. Introduction

OPTICAL access networks are in widespread use, and so it is essential that we are capable of providing in-service upgrades or additional services without affecting any existing services. Optical code division multiple access (OCDMA) [1]–[12], [16], [17] has attracted attention because its signature codes allow us to meet the above requirements. Orthogonal spectral amplitude coding optical code division multiple access (SAC OCDMA) [2]–[8] is particularly desirable as regards realizing a simple and cost-effective transmitter on user premises. However, its maximum number of multiplexed signal lights is restricted by accumulated multiple-access interference (MAI) and beat noise. MAI can be suppressed by using orthogonal codes and differential detection [2]–[8].

The beat noise increases in proportion to the square of the number of multiplexed signal lights and is a factor limiting system capacity [1]–[3]. Several schemes have been proposed to overcome this limit [4]–[7]. Unfortunately, most of these schemes use particular kinds of code sequences that exhibit fewer coincidences between the "1" chips of the two codes such as spectral amplitude code sequences with an additional temporal coding [4] and code sequences containing fewer "1" chips [5], [6]. As a scheme that is applicable to any orthogonal spectral code sequences, we have proposed the use of coherent detection with local light [7]. In our scheme, a sufficiently strong local light amplifies the signal intensity without increasing the beat noise between multiplexed signal lights. Although our previous paper reported the first demonstration of homodyne detection with a spectral coding OCDMA scheme to mitigate the beat noise, it did not provide any analysis.

In this paper, we clarify the requirements for applying coherent detection to the SAC OCDMA scheme. We then analyze the applicability of the coherent detection technique theoretically by using both a strong local light and an intermediate frequency filter for heterodyne envelope detection. From our analysis, we confirm experimentally the system requirements and the mitigation of the beat noise. The experimental results agree with the analysis, and this indicates sufficient potential for any orthogonal spectral code sequences to reduce the limit caused by beat noise.

This paper is organized as follows. In Section II, we describe the SAC OCDMA system with heterodyne detection and analyze its performance theoretically. In Section III, we confirm our Section II analysis experimentally. Section IV presents our conclusions.

II. Theoretical Analysis of SAC OCDMA System With Heterodyne Detection

A. System Configuration With Heterodyne Detection

We investigate a configuration incorporating heterodyne envelope detection as one configuration providing greater mitigation of the beat noise effect than a configuration with homodyne detection. This system has two key features. First, the light source provides a local light with sufficiently high power to make the beat noise between multiplexed signal lights negligible. Second, a band pass filter (BPF) acting as an intermediate frequency filter removes the beat noise and the direct detection components.

A simplified system model and the frequency relationships between signal and local lights are shown in Figs. 1 and 2, respectively. Here, the codes "1100" and "1010" are used as an example. A signal light is composed of several optical frequency chips. The encoding is performed in a unipolar (1, 0) manner. The chips are encoded with a coder, which selectively passes chips that have been assigned a value of 1 by the code that is being used. The signal lights from the coders are multiplexed at a star coupler and then reach the decoders in the receivers. The signal lights are coupled with local light. Here the signal and local light chips have the same frequency separation F, as shown in Fig. 2. The frequency separation F is wide enough for the beat noise of chips with different numbers to lie outside the receiver's bandwidth. The frequencies of the respective local light chips differ from those of the signal lights with an intermediate frequency (IF) f_{IF}. Signal

Manuscript received September 27, 2007; revised December 19, 2007.

The authors are with Access Network Service Systems Laboratories, NTT Corporation, Chiba 261-0023, Japan (e-mail: mana@ansl.ntt.co.jp; kaneko.shin@ansl.ntt.co.jp; taniguti@ansl.ntt.co.jp; noriki@ansl.ntt.co.jp; kumozaki@ansl.ntt.co.jp; imai@kanagawa-u.ac.jp; yosimoto@ansl.ntt.co.jp; tsubokawa.makoto@ansl.ntt.co.jp).

Digital Object Identifier 10.1109/JLT.2008.917369

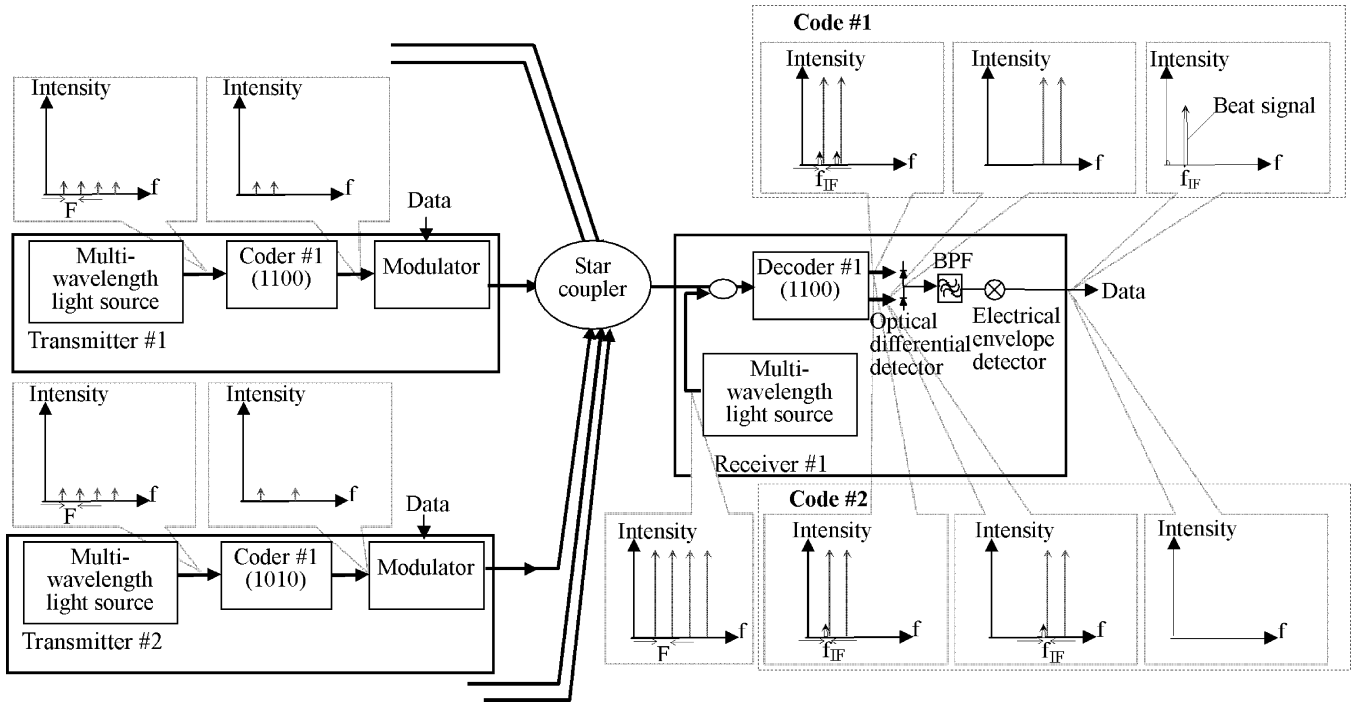

Fig. 1. System configuration with heterodyne detection.

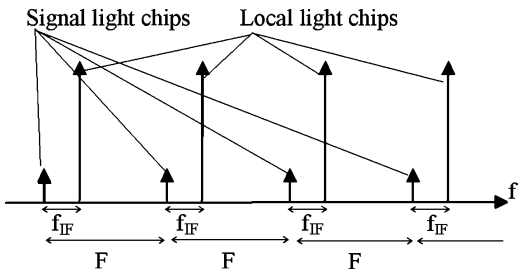

Fig. 2. Frequency relationship between signal and local lights.

and local lights pass through the decoder to an optical differential detector. Here, the decoder for each code is composed of a pair of optical filters matched to the targeted code, and it passes the light from both filters to the inputs of an optical differential detector. The decoding is performed in a bipolar $(1, -1)$ manner in the electrical domain. A matched decoder passes all received "1" chips to one of the two photodiodes that form the optical differential detector. An unmatched decoder divides the chips between the photodiodes of the optical differential detector to balance their output. This balancing out after differential detection results from the characteristics of the code set, and it ensures that signal lights are orthogonal to each other. Hadamard code sequences and cyclic shifted maximum length sequences are typical examples of such orthogonal code sets [2], [4] and they are also code sets that exhibit the largest coincidences between the "1" chips of two codes. Thus, they are good examples for examining the application of our scheme to any orthogonal spectral code sequence. The orthogonal property of a Hadamard code sequence means that for any pair of codes, the number of chips in agreement is equal to the number in disagreement as follows:

$$\sum_{n=1}^{N} C_{kn}C_{in} = \begin{cases} N/2 & (k=i) \\ N/4 & (k\neq i) \end{cases}$$
$$\sum_{n=1}^{N} C_{kn}C'_{in} = \begin{cases} 0 & (k=i) \\ N/4 & (k\neq i), \end{cases} \quad (k,i\in 1,2,\ldots,K) \tag{1}$$

where C_{in} and C'_{in} are the value and the complementary value of the nth chip ($n = 1$ to N; n is the chip number, N is the total number of chips) of the ith code (i and $k = 1$ to K; i and k are the code numbers, K is the total number of codes). Here, each code is constructed by taking one row (except for the first row) of the Hadamard matrix of order 2^{N}. The orthogonal property or the balancing out of the unmatched signals is destroyed by the imbalance between the intensity of the optical frequency chips [2] and the imperfect filtering of the decoder chips. In this system, except for the IF signal, electrical signals, output by the optical differential detector are filtered out by the BPF. The IF signal is demodulated at an electrical envelope detector.

The IF signal is mainly degraded by the MAI and the receiver noises rather than by the beat noise unlike the direct detection systems. If all the signal lights are present at a given instant, the received optical field in front of the decoder is

$$E_k = D_k(t)\sum_{n}^{N} E_{kn}\cos(2\pi f_{kn}t + \phi_{kn}) \tag{2}$$

where $D_k(\mathrm{t})$ is the data value of the kth signal light at time t and its value is 1 or 0. E_{kn}, f_{kn} and ϕ_{kn} are the amplitude, the optical frequency and the phase noise of the nth chip of the kth signal light, respectively. Here, the frequencies of the same numbered chips of all signal lights are assumed to be the same

as are the polarization states of all signal lights (the worst case scenario). Each signal light is considered to have equal power at the receivers and its temporal waveform is assumed to be constant over the bit duration for simplicity. Before demodulation by the electrical envelope detector, the current i_p for the pth code is defined as

$$\begin{aligned}
i_p =& RD_p(t)\sum_{n}^{\mathrm{N}}\left(C_{pn}-C'_{pn}\right)E_{pn}E_{Ln}\\
&\times\cos(2\pi f_{\mathrm{IF}}t+\phi_{pn}-\phi_{Ln})\\
&+R\sum_{k;k\neq p}^{\mathrm{K}}D_k(t)\sum_{n}^{\mathrm{N}}\left(C_{pn}-C'_{pn}\right)E_{kn}E_{Ln}\\
&\times\cos(2\pi f_{\mathrm{IF}}t+\phi_{kn}-\phi_{Ln})\\
&+O_{bpf}\left\{\frac{1}{2}RD_p(t)\sum_{n}^{\mathrm{N}}\left(C_{pn}-C'_{pn}\right)E_{pn}^2\right.\\
&\quad+\frac{1}{2}R\sum_{k;k\neq p}^{\mathrm{K}}D_k(t)\sum_{n}^{\mathrm{N}}\left(C_{pn}-C'_{pn}\right)E_{kn}^2\\
&\quad+\frac{1}{2}R\sum_{n}^{\mathrm{N}}\left(C_{pn}-C'_{pn}\right)E_{Ln}^2\\
&\quad+R\sum_{k;k\neq p}^{\mathrm{K}}D_p(t)D_k(t)\sum_{n}^{\mathrm{N}}\left(C_{pn}-C'_{pn}\right)\\
&\quad\times E_{pn}E_{kn}\cos(\phi_{pn}-\phi_{kn})\\
&\quad+R\sum_{i;i\neq k,p}^{K}\sum_{k;k\neq p}^{K}D_i(t)D_k(t)\sum_{n}^{\mathrm{N}}\left(C_{pn}-C'_{pn}\right)\\
&\quad\left.\times E_{in}E_{kn}\cos(\phi_{in}-\phi_{kn})\right\}+n(t)\\
=&D_p(t)i_{\mathrm{data}}+\varsigma\sum_{k;k\neq p}^{K}D_k(t)i_{\mathrm{data}}\\
&+O_{bpf}\left\{\frac{D_p(t)i_{\mathrm{data}}}{2\sqrt{lr}}+\frac{\xi\sum_{k;k\neq p}^{\mathrm{K}}D_k(t)i_{\mathrm{data}}}{2\sqrt{lr}}+\xi\sqrt{lr}i_{\mathrm{data}}\right.\\
&\quad+\frac{\sum_{k;k\neq p}^{\mathrm{K}}D_p(t)D_k(t)i_{\mathrm{data}}}{2\sqrt{lr}}\\
&\quad\left.+\frac{\xi\sum_{i;i\neq k,p}^{K}\sum_{k;k\neq p}^{K}D_i(t)D_k(t)i_{\mathrm{data}}}{2\sqrt{lr}}\right\}+n(t)\\
\approx&D_p(t)i_{\mathrm{data}}+\varsigma\sum_{k;k\neq p}^{\mathrm{K}}D_k(t)i_{\mathrm{data}}+n(t),\\
&i_{\mathrm{data}}\equiv R\sum_{n}^{\mathrm{N}}\left(C_{pn}-C'_{pn}\right)E_{pn}E_{Ln}. \qquad (3)
\end{aligned}$$

R is the detector responsivity, C_{pn} and C'_{pn} are the power transmission function of the nth chip of the respective filters of the pth decoder. Here C_{pn} and C'_{pn} ideally have the same value in (1). E_{Ln} and ϕ_{Ln} are the amplitude and phase noise of the nth chip of the local light, respectively. $n(t)$ is the receiver noise. i_{data} is the current intensity of the targeted signal, O_{bpf} is the rejection ratio of the BPF, and lr is the ratio of the intensity of one local light chip to that of the signal light. ς is the crosstalk ratio of the MAI. ξ is the ratio of the residual direct detection components of an untargeted signal light to the targeted signal light, which is the same as the crosstalk ratio in conventional detection systems. This ratio is usually defined as follows:

$$\xi\equiv\frac{\sum_{n}^{N}\left(C_{pn}-C'_{pn}\right)E_{kn}^2}{\sum_{n}^{N}\left(C_{pn}-C'_{pn}\right)E_{pn}^2} \qquad (4)$$

and is negligible. In (3), the first and second terms are the targeted signal and the MAI of the untargeted signals, which are beat signals between the signal and local lights, respectively. The third, fourth, and fifth terms are the direct detection components of the targeted and untargeted signal lights and the local light, respectively. The sixth and seventh terms are the primary targeted–untargeted signal beat noise (the primary beat noise) and the secondary untargeted–untargeted signal beat noise (the secondary beat noise), respectively. Here we assume a uniform phase difference condition where the phase differences between the respective chips of the signals and local lights are uniform and defined as

$$\phi_{kn}-\phi_{Ln}=\phi_{km}-\phi_{Lm}\,(1\leq n,m\leq N,k\in(1,\ldots,K)). \qquad (5)$$

From (5), the phase differences between the respective chips of the signal lights are also uniform when (5) is true for all signal lights. In the uniform phase difference condition, all the values of the cosine functions of the beats between the respective chips of the signal and local lights in (3) are the same. Under this condition, the ratio of the crosstalk of the MAI to the beat signal is minimized and is defined as follows:

$$\varsigma\equiv\frac{\sum_{n}^{N}\left(C_{pn}-C'_{pn}\right)E_{kn}E_{Ln}}{\sum_{n}^{N}\left(C_{pn}-C'_{pn}\right)E_{pn}E_{Ln}}. \qquad (6)$$

On the other hand, in the nonuniform phase difference condition, the values of the cosine functions vary from -1 to 1, and the MAI is not always balanced out despite the orthogonal property of the code sets.

When a strong local light is used, the third, fourth, sixth, and seventh terms are diminished compared with the beat signal and MAI by the square root of lr. Furthermore, the third to seventh terms are rejected by the BPF. Thus, it is assumed that the MAI is dominant over the beat noise and direct detection component at high lr and low O_{bpf} values. When the noises are assumed to be independent, the noise variance σ^2 is

$$\sigma^2=\overline{i_s^2}+\overline{i_b^2}+\overline{i_L^2}+\overline{i_{MAI}^2}+\overline{i_{s-b}^2}+\overline{i_{b-b}^2}+\overline{i_c^2} \qquad (7)$$

where $\overline{i_s^2}$, $\overline{i_b^2}$, $\overline{i_L^2}$, $\overline{i_{MAI}^2}$, $\overline{i_{s-b}^2}$, $\overline{i_{b-b}^2}$, and $\overline{i_c^2}$ are the shot noises of the targeted and untargeted signal lights and local light, the

MAI, the primary and secondary beat noises, and the receiver noise, respectively.

B. Requirements for Heterodyne Detection System

We clarify two requirements for the application of coherent detection to SAC OCDMA in relation to mitigating the beat noise. One is that the signal intensity must increase without increasing the beat noise. The other is that we must satisfy (5); namely, that the phase differences of the respective optical frequency chips that form parts of the signal and local lights must be uniform. In particular, the latter requirement has not been described in earlier studies of coherent detection such as coherent detection in a multiwavelength communication system [13] and temporal coding OCDMA [9]–[11], [17].

The requirements are described below.

1) High Signal-to-Beat Noise Ratio: There are two ways to realize the first requirement where a beat signal is insensitive to beat noise. One is that the optical power of the local light is high enough for the beat noise of the signal lights to be negligible compared with the beat signal. The intensity of the beat noise in the uniform phase difference condition is approximated by $(K-1)i_{\rm data}/2\sqrt{lr}$. For instance, the optical power of the local light is required to be at least 40 dB higher than the total power of the signal lights from the transmission line in order to suppress the beat noise to 20 dB lower than the beat signal. The other is to reject the beat noise between signals by using a BPF with heterodyne detection. This can compensate for the shortfall of the power of the local light. Our experiment employs a BPF that rejects more than 20 dB at the stop-band.

2) Uniform Phase Difference: The uniform phase difference condition is required both to ensure the intensity of the targeted signal and to maintain the orthogonality between signals. For simplicity, we assume that only one targeted or untargeted signal light is transmitted. The current demodulated by the electrical envelope detector is proportional to the square of the intensity of the current i_p, and then its high-frequency component is filtered out by a low-pass filter. The output of the low-pass filter i_{p2} is expressed as

$$i_{p2} \approx R^2 D_k^2(t) \sum_n^N \sum_m^N \left(C_{pn} - C'_{pm}\right) E_{kn} E_{Ln} \left(C_{pm} - C'_{pm}\right) \times E_{km} E_{Lm} \cos\left((\phi_{kn} - \phi_{Ln}) - (\phi_{km} - \phi_{Lm}) - 2\pi f_{\rm IF} DL_{nm}\right). \tag{8}$$

Here DL_{nm} is the relative delay between the nth and mth chips. This delay is caused by their path difference from their branch point to the adder-subtractor in the optical differential detector. The difference should be reduced to a negligible one, for example, with several gigahertz intermediate frequencies, submillimeter accuracy is required to obtain a sufficiently small crosstalk ratio for the MAI. With a negligible path difference, the uniform phase difference makes all the phases of the cosine functions in (8) zero. Otherwise i_{p2} is varied from 0 to $i_{\rm data}^2$ from (1) and (8). With a uniform phase difference, i_{p2} for the targeted signal light reaches $i_{\rm data}^2$ and i_{p2} for an untargeted one, namely the MAI, is 0. Thus, the uniform phase difference is required both to ensure the intensity of the targeted signal and to guarantee the orthogonality of SAC OCDMA with coherent detection.

Next, we show that the noise variance σ^2 is also increased by the nonuniform phase differences. The respective noise variances σ^2 and $\sigma_{\rm nu}^2$ for uniform and nonuniform phase differences between the untargeted signal and local lights are expressed as

$$\begin{aligned}\sigma^2 &\approx \overline{i_L^2} + \overline{i_{MAI}^2} + \overline{i_{s-b}^2} + \overline{i_{b-b}^2} + \overline{i_c^2} \\ &= 2eBR_L\sqrt{lr} i_{\rm data} + \frac{1}{2}(K-1)\varsigma^2 i_{\rm data}^2 \\ &\quad + O_{bpf}^2 \left\{ \frac{(K-1)}{8lr} i_{\rm data}^2 + \frac{(K-1)(K-2)}{16lr} \xi^2 i_{\rm data}^2 \right\} \\ &\quad + \overline{i_c^2} \\ &\approx \frac{1}{2}(K-1)\varsigma^2 i_{\rm data}^2 + \overline{i_c^2} \end{aligned} \tag{9}$$

$$\begin{aligned}\sigma_{nu}^2 &\approx \overline{i_L^2} + \overline{i_{MAI}^2} + \overline{i_{s-b}^2} + \overline{i_{b-b}^2} + \overline{i_c^2} \\ &= 2eBR_L\sqrt{lr} i_{\rm data} + \frac{1}{2N}(K-1) i_{\rm data}^2 \\ &\quad + O_{bpf}^2 \left\{ \frac{(K-1)}{8Nlr} i_{\rm data}^2 + \frac{(K-1)(K-2)}{16Nlr} i_{\rm data}^2 \right\} \\ &\quad + \overline{i_c^2} \\ &\approx \frac{1}{2} i_{\rm data}^2 + \overline{i_c^2}. \end{aligned} \tag{10}$$

e is an elementary electric charge, B is the electrical bandwidth of the receiver, and R_L is the load resistance of the optical differential detector. Here. the shot noise of the signal lights is negligible compared with the local light. The phase differences of the targeted signal and local lights are assumed to be uniform in both cases. The number of multiplexed signal lights is assumed to be approximately the total number of chips N. When the phase differences are uniform, the MAI in (9) is negligible because the crosstalk ratio is assumed to be negligible. By contrast, as shown in (10), the MAI is not negligible in the nonuniform case.

Next, we explain the assumption of the balancing out of the secondary beat noise in (9). From (1), half of the "1" chips of any combination of two untargeted signal lights coincide and they are divided evenly between the two photodiodes of the optical differential detector. Thus, their beat noises at both photodiodes are balanced out under the uniform phase difference condition.

To realize a uniform phase difference condition, we can use multiwavelength lights with uniform phase noise. Candidates for a light source with a uniform phase include a mode locked laser [12] and a light source that employs modulation to generate sidebands [8], [15]. The former is widely used in OCDMA schemes and its structure is almost the same as that of an electro-absorption distributed feedback laser diode, which is currently utilized for low-cost metro access. Thus, it can be mass produced inexpensively. A loop-back scheme that will allow a number of coders to share the light source will also drive down the system cost [12]. Moreover, these light sources allow us to replace a complex assembly of multiple frequency control systems with one frequency control circuit.

Also note that we assumed that the OCDMA signals are transmitted in the zero-dispersion region of the transmission fiber or that the fiber dispersion is compensated.

C. BER Expressions of Heterodyne Detection System

This subsection analytically formulates the bit error rate (BER) performance to confirm the effectiveness of heterodyne detection systems by comparison with experimental results. Using a similar derivation to that in [14], the current i_p in (3) is expressed in (11), shown at the bottom of the page, where r^2 is the envelope. ϕ'_k is the phase and is assumed to be π (the worst MAI case). A and z are the signal and MAI amplitudes, respectively. x and y are the amplitudes of the in-phase and quadrature components of the noise, respectively. A' is the amplitude of the signal with MAI in the worst case, and x' is the amplitude of the in-phase component of the noise with A'. The probability density function of z is approximated by

$$p(z) = \sum_{u=0}^{K-1} \frac{{}_{K-1}C_u}{2^{K-1}} \delta(z + u\varsigma A) \tag{12}$$

where u is the number of untargeted signals whose data values are marks. The joint distribution given z is

$$\begin{aligned} p_z(r) &= \int_0^{2\pi} \frac{r}{2\pi N} \exp\left(-\frac{r^2 + A'^2 - 2rA'\cos\theta}{2N}\right) d\theta \\ &= \frac{r}{N} I_0\left(\frac{rA'}{N}\right) \exp\left(-\frac{r^2 + A'^2}{2N}\right) \\ I_0(v) &= \frac{1}{2\pi} \int_0^{2\pi} \exp(v\cos\theta) d\theta \end{aligned} \tag{13}$$

where $I_0(v)$ is the modified Bessel function of the first kind and zeroth order. The BER is

$$\begin{aligned} BER &= \frac{1}{2}\left[\int_0^T \int_{-\infty}^{\infty} p(z)p_z(r)dzdr + \int_T^{\infty} \int_{-\infty}^{\infty} p(z)p_z(r)dzdr\right] \\ &= \sum_{u=0}^{K-1} \frac{{}_{K-1}C_u}{2^{K-1}} \left[1 - Q\left(\frac{A - u\varsigma A}{\sigma}, \frac{T}{\sigma}\right)\right. \\ &\qquad \left. + Q\left(\frac{|u\varsigma A|}{\sigma}, \frac{T}{\sigma}\right)\right], \\ Q(a,b) &= \int_{-\infty}^{\infty} tI_0(at) \exp\left(-\frac{t^2 + a^2}{2}\right) dt,\ T = A/2 \end{aligned} \tag{14}$$

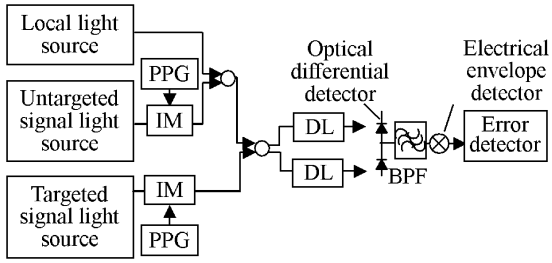

Fig. 3. Experimental setup in Section III-A.

where $Q(a,b)$ and T are Marcum's Q-function and the threshold level of a mark and a space, respectively. When the number of multiplexed signal lights is sufficient to be approximated as a Gaussian distribution, the BER can be additionally approximated by

$$BER \approx \frac{1}{2} \exp\left(-\frac{1}{8} \frac{i_{\mathrm{data}}^2}{\sigma^2 + (K-1)\varsigma^2 i_{\mathrm{data}}^2/2}\right) \tag{15}$$

where $(K-1)\varsigma^2 i_{\mathrm{data}}^2/2$ is the variance of the MAI current.

Using (14), we conducted an experiment to confirm that the BER performance of the heterodyne detection system is degraded by the MAI rather than the beat noise, unlike direct detection systems.

III. Experiment

We describe two experiments. The experiment described in Section III-A is designed to confirm the requirements of this scheme. The experiment in Section III-B shows that the beat noise is mitigated in a heterodyne detection system.

A. Confirmation of Requirements

Here, we designed the principle experiment to confirm two requirements. The first requirement is that the beat noise is small enough to be ignored when compared with the beat signal. The second requirement is that the uniform phase difference condition balances out the MAI and the secondary beat noise.

For confirmation, the local and untargeted signal lights were coupled with the targeted signal light at a 2×2 optical coupler where each output was connected to both inputs of an optical differential detector as shown in Fig. 3. This setup balanced out the direct detection components and the MAI between the untargeted signal and local lights and left the beat signal between the targeted signal and local lights and the primary beat noise

$$\begin{aligned} i_p &\approx r\cos(2\pi f_{\mathrm{IF}} t + \theta + \phi_{pn} - \phi_{Ln}) \\ r^2 &\equiv \left(A\sqrt{\left(D_p(t) + \varsigma \sum_{k;k\neq p}^{k} D_k(t)\cos\phi'_k\right)^2 + \left(\varsigma \sum_{k;k\neq p}^{k} D_k(t)\sin\phi'_k\right)^2} + x\right)^2 + y^2 \\ &\approx (AD_p(t) - z + x)^2 + y^2 \equiv (A' + x)^2 + y^2 \equiv x'^2 + y^2, \\ \phi'_k &\equiv \phi_{kn} - \phi_{pn},\ z \equiv A\varsigma \sum_{k;k\neq p}^{K} D_p(t),\ \theta \equiv \tan^{-1}(y/x') \end{aligned} \tag{11}$$

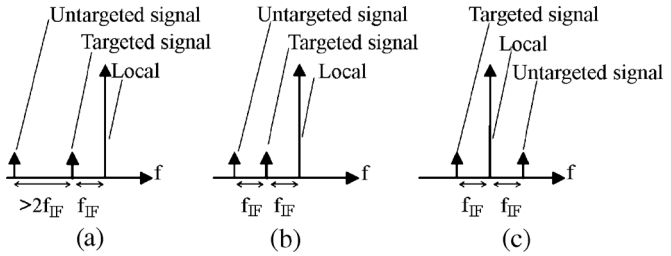

Fig. 4. Spectral arrangement for different types of noise. (a) Only shot noise. (b) Signal-signal beat. (c) Signal-local beat.

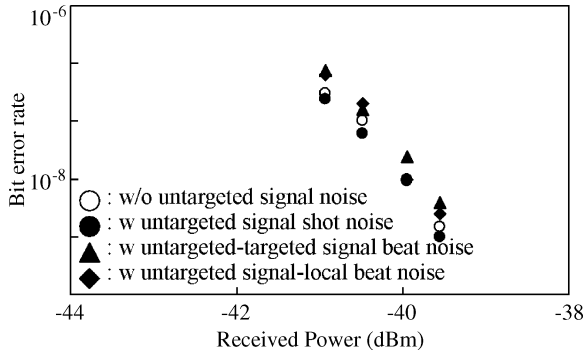

Fig. 5. BER versus received power for various types of noise.

between the targeted and untargeted signal lights at the optical differential detector. The optical powers of the local and untargeted signal lights were 0 and -25 dBm at the inputs of the optical differential detector, respectively. Here, the power of the local light is 40 dB higher than that of the targeted signal light. The power of the untargeted signal light is designed to emulate 32 untargeted signal lights. Both signal lights were modulated by intensity modulators (IM) at a bit rate of 1 Gbit/s with a 2^7-1 pseudorandom binary sequence (PRBS) pattern from pulse pattern generators (PPG). The IF components ($f_{\rm IF} = 2.5$ GHz) of the output of the optical differential detector passed through a BPF (pass band $= 1.25$ to 3.75 GHz) and were demodulated by an electrical envelope detector. As shown in Fig. 4, the spectrum arrangements between the three lights were set so that only the intended beats would pass. The beat signal passed through the BPF for all arrangements. Fig. 4(a) and (b) were set for the first requirement. Fig. 4(a) shows an example with only untargeted signal shot noise where beats other than the beat signal did not pass. This confirms that the beat noise was removed by using a BPF with heterodyne detection. Fig. 4(b) shows an example with the primary beat noise where the frequency difference between the two signal lights was $f_{\rm IF}$ for the comparison between the beat signal and the beat noise without the BPF rejection. Fig. 4(c) was set for the second requirement. It shows an example with the MAI where the frequency difference between the untargeted signal and local lights was $f_{\rm IF}$. This confirms that the MAI was balanced out when the phase difference was uniform. Here the phase difference between the untargeted signal and the local lights at both inputs of the differential detector was the same because they were split after being coupled. The path difference between the split lights was matched using a variable optical delay line (DL). Moreover, if the local light and the MAI were assumed to be an untargeted signal light and the secondary beat noise, respectively, this was also used to confirm that the simulated secondary beat noise was balanced out when the phase difference was uniform. Fig. 5 shows the BER of the targeted signal light without and with an untargeted signal light. The unfilled symbols show results obtained without the untargeted signal light; the filled circles, triangles, and diamonds show results obtained with the untargeted signal shot noise, the primary beat noise, and the MAI, respectively. The BER plots in Fig. 5 show that all the results almost coincide and there is no BER degradation. This shows that the beat noise is small enough to be negligible compared with the beat signal. This also shows that the MAI and the secondary beat noise can be balanced out when the phase differences are uniform, or else the MAI of the untargeted signal with 15 dB higher power will degrade the BER of the targeted signal.

As shown in this subsection, the beat noise is small compared with the beat signal between the signal and local lights. The uniform phase difference suppresses the MAI and the secondary beat noise.

B. Confirmation of Reduction in Beat Noise

This subsection confirms that the beat noise is reduced below the MAI as shown in (14). The experimental configuration is shown in Fig. 6. The multiwavelength light sources with uniform phase noise consisted of a distributed feedback laser diode (LD), an IM to yield a double sideband, and a 12.5-GHz synthesizer to drive the modulator, which generated three lights with 12.5-GHz separation. The signal lights were modulated in the transmitters at a bit rate of 1 Gbit/s with a 2^7-1 PRBS pattern from the PPGs. As shown by the spectra in Figs. 7(a) and 8(a), the targeted and untargeted signal lights were coded as "0011" and "0101" using a Mach–Zehnder interferometer with free spectral ranges (FSR) of 40 and 20 GHz, respectively. In the receiver, the signal lights were coupled with the local light. The frequency differences between the chips forming the signal and local lights were 2.5 GHz. The spectrum of the local light is shown in Fig. 9(a). The coupled lights were divided and input via optical filters with a 25-GHz channel spacing into an optical differential detector, which functioned as a decoder. Here, the path difference between the divided lights was matched using a variable optical delay line. The spectra of the signal and local lights input into the differential detector are shown in Figs. 7(b) and (c), 8(b) and (c), and 9(b) and (c). The output of the optical differential detector was filtered by a BPF (pass band $= 1.25$ to 3.75 GHz), and demodulated by an electrical envelope detector. The measured square value of the crosstalk ratio of the MAI, which reflects the imbalance between the chips, was -30.7 dB. Fig. 10(a) and (b) show the low-pass filter output after the electrical envelope detector for the targeted signal light and the untargeted signal light, whose power is 10 dB higher than that of the targeted one, respectively. As shown in Fig. 10, the decoding is successful. Fig. 11 shows the BER of the targeted signal light without and with untargeted signal light. The bold and thin solid lines show the BER calculated according to (14) with untargeted signal light at powers of 0 and 10 dB higher, respectively. The unfilled symbols show results obtained without untargeted signal light;

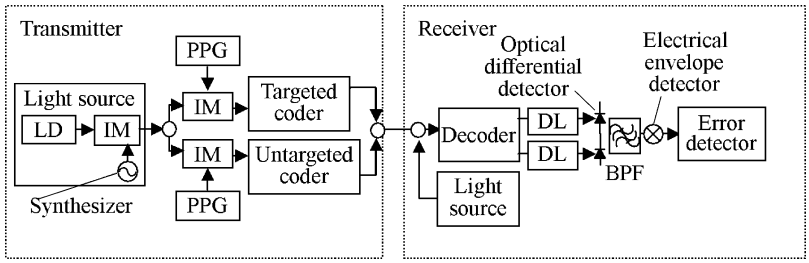

Fig. 6. Experimental setup in Section III-B.

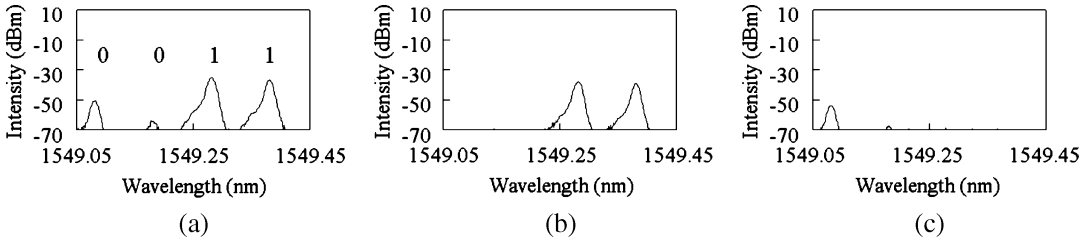

Fig. 7. Spectra of targeted signal light. (a) Decoder input. (b) Upper detector. (c) Lower detector.

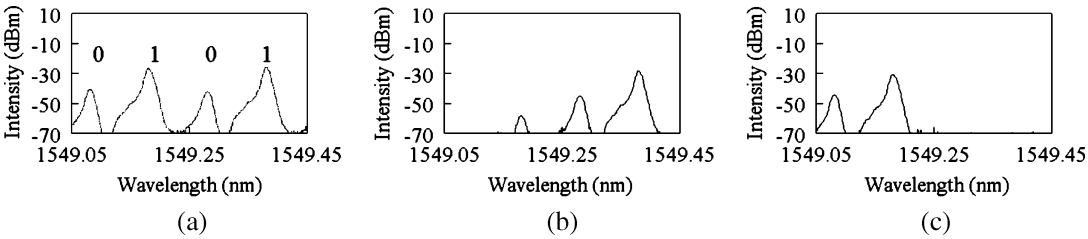

Fig. 8. Spectra of untargeted signal light. (a) Decoder input. (b) Upper detector. (c) Lower detector.

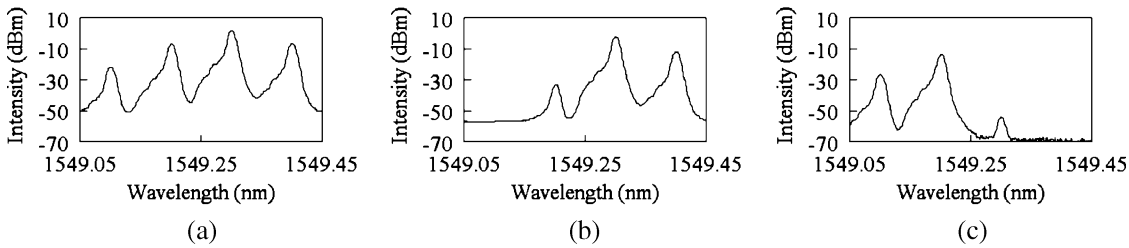

Fig. 9. Spectra of local light. (a) Decoder input. (b) Upper detector. (c) Lower detector.

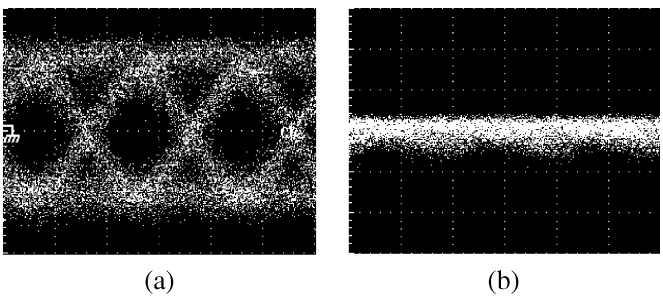

Fig. 10. Output of electrical envelope detector. (a) Targeted signal. (b) Untargeted signal.

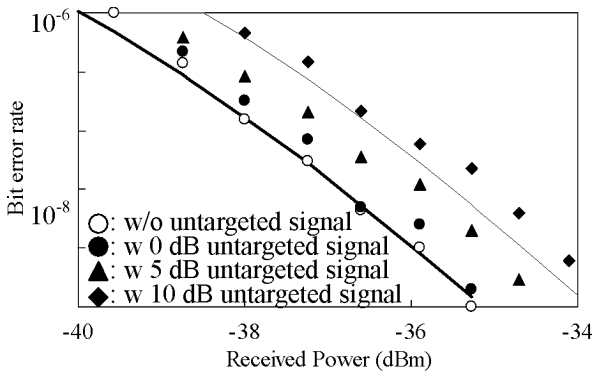

Fig. 11. BER versus received power.

the solid circles, triangles, and diamonds show results obtained with untargeted signal light and with powers that were 0, 5, and 10 dB higher than that at a BER of 10^{-9} to emulate multiple untargeted signal lights. Here, the multiple untargeted signal lights can be simulated by the increase in the power of untargeted signal light as shown in (9) and (15). Fig. 12 shows the power penalty at a BER of 10^{-9} as a function of the number of multiplexed signal lights. In Fig. 12, the thin and bold black and gray lines show the penalty calculated using (14) for values of -25, -30.7, and -35 dB, respectively. The solid symbols show

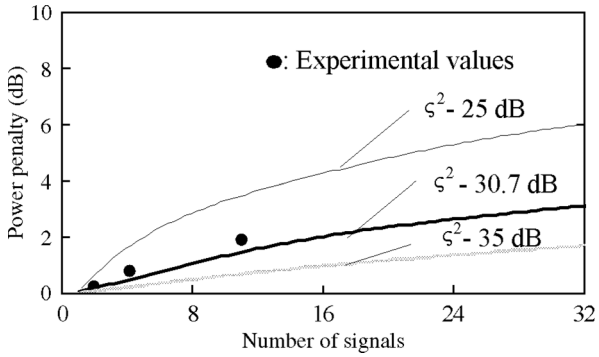

Fig. 12. Power penalty versus number of signals.

the results obtained with the untargeted signal light at powers of 0, 5, and 10 dB. The values used in the calculations were the values measured in the experimental setup. The solid symbols in Fig. 12 approximately agree with the bold black line, which was degraded by the MAI in relation to the measured value of $\varsigma^2 - 30.7$ dB. Thus, there is no degradation caused by the beat noise. The BER evaluation confirms that the beat noise is negligible compared with the experimentally obtained MAI.

As shown in Figs. 11 and 12, the estimation provided by (14) approximately agrees with the measured results; the performance is not degraded by the beat noise. The estimation provided by (15) also approximately agrees with the measured results.

In this experiment, we demonstrate the applicability of a heterodyne detection system using code sets that coincide at half of "1" chips; this indicates sufficient potential to reduce the limit caused by beat noise for any orthogonal spectral code sequences.

IV. Conclusion

In order to mitigate beat noise, we investigated the applicability of a heterodyne detection technique to a spectral amplitude coding optical code division multiple access scheme. We clarified the system requirements and determined analytically that the optical frequency chips forming parts of the signal and local lights require uniform phase differences even for envelope detection. We also confirm this investigation with an optical code division multiple access experiment and the results are in good agreement. A BER evaluation of the experimental results using one of the severest beat noise code sequences proves that the limit caused by the beat noise is negligible.

Acknowledgment

The authors would like to thank H. Shinohara for his encouragement. They would also like to thank S. Narikawa and H. Sanjoh for invaluable discussions.

References

[1] A. Stock and E. H. Sargent, "The role of optical CDMA in access networks," *IEEE Commun. Mag.*, vol. 40, no. 9, pp. 83–87, Sep. 2002.

[2] D. Zaccarin and M. Kavehrad, "An optical CDMA system based on spectral encoding of LED," *IEEE Photon. Technol. Lett.*, vol. 4, no. 5, pp. 479–482, Apr. 1993.

[3] E. D. J. Smith, P. T. Gough, and D. P. Taylor, "Noise limits of optical spectral-encoding CDMA systems," *Electron. Lett.*, vol. 31, no. 17, pp. 1469–1470, Aug. 1995.

[4] E. D. J. Smith, R. J. Blaikie, and D. P. Taylor, "Performance enhancement of spectral-amplitude-coding optical CDMA using pulse-position modulation," *IEEE Trans. Commun.*, vol. 46, no. 9, pp. 1176–1185, Sep. 1998.

[5] X. Zhou, H. M. H. Shalaby, C. Lu, and T. Cheng, "Code for spectral amplitude coding optical CDMA systems," *Electron. Lett.*, vol. 36, pp. 728–729, Apr. 2000.

[6] Z. Wei and H. Ghafouri-Shiraz, "Codes for spectral-amplitude-coding optical CDMA systems," *J. Lightw. Technol.*, vol. 20, no. 8, pp. 1284–1291, Aug. 2002.

[7] S. Kaneko and N. Miki, "Optical OFCDM systems for beat-noise suppression and high frequency efficiency," *Proc. 2007 IEICE General Conf.*, 2007, B-10-23.

[8] M. Yoshino, S. Kaneko, and N. Miki, "Multi-wavelength light source for OCDMA using a directly sinusoidally modulated laser diode," in *Proc. OFC'07*, Mar. 2007, JThA31.

[9] N. Wada and K. Kitayama, "Error-free 10 Gbit/s transmission of coherent optical code division multiplexing using all-optical encoder and balanced detection with local code," in *Proc. OFC '98*, Mar. 1998, FE7.

[10] W. Huang and I. Andonovic, "Coherent optical pulse CDMA Systems based on coherent correlation detection," *IEEE Trans. Commun.*, vol. 47, no. 2, pp. 261–271, Feb. 1999.

[11] N. Wada and K. Kitayama, "A 10 Gb/s optical code division multiplexing using 8-chip optical bipolar code and coherent detection," *J. Lightw. Technol.*, vol. 17, no. 10, pp. 1758–1764, Aug. 1999.

[12] K. Kitayama, X. Wang, and N. Wada, "OCDMA over WDM PON-solution path to gigabit-symmetric FTTH," *J. Lightw. Technol.*, vol. 24, no. 4, pp. 1654–1662, Apr. 2006.

[13] L. G. Kazovsky, "Multichannel coherent communications systems," *J. Lightw. Technol.*, vol. LT-5, no. 8, pp. 1095–1102, Aug. 1987.

[14] T. Okoshi and K. Kikuchi, *Coherent Optical Fiber Communications*. Norwell, MA: Kluwer, 1988.

[15] R. P. Scott, N. K. Fontaine, J. P. Heritage, B. H. Kolner, and S. J. B. Yoo, "3.5-THz wide, 175 mode optical comb source," in *Proc. OFC'07*, Mar. 2007, OWJ3.

[16] M. M. Karbassian and H. Ghafouri-Shiraz, "Fresh prime codes evaluation for synchronous PPM and OPPM signaling for optical CDMA networks," *J. Lightw. Technol*, vol. 25, no. 6, pp. 1422–1430, Jun. 2007.

[17] M. M. Karbassian and H. Ghafouri-Shiraz, "Performance analysis of coherent optical CDMA using a novel Prime code family," *J. Lightw. Technol*, vol. 25, no. 10, pp. 3028–3034, Oct. 2007.

Manabu Yoshino received the B.S. and M.S. degrees in physics from Waseda University, Tokyo, Japan, in 1991 and 1993, respectively.

Since joining NTT in 1993, he has been mainly engaged in R&D of optical access systems.

Mr. Yoshino is a member of the Institute of Electronics, Information, and Communication Engineers of Japan (IEICEJ).

Shin Kaneko received the B.E. and M.E. degrees in electronics engineering from the University of Tokyo, Tokyo, Japan, in 2002 and 2004, respectively.

Since joining NTT in 2004, he has been engaged in research on optical multiplexing technologies for optical access systems.

Mr. Kaneko is a member of IEICEJ.

Tomohiro Taniguchi received the B.E. and M.E. degrees in precision engineering from the University of Tokyo, Tokyo, Japan, in 2000 and 2002, respectively.

Since joining NTT in 2002, he has been engaged in research on optical-access systems, mainly related to optical heterodyne technique and radio-on-fiber transmission.

Mr. Taniguchi is a member of the IEICEJ.

Noriki Miki (M'92) received the B.E. and M.E. degrees in electronics engineering from Shinshu University, Nagano, Japan, in 1982 and 1984, respectively.

He joined NTT in 1984 and was engaged in R&D of digital subscriber loop transmission systems. Since 1991, he has worked on R&D of fiber optic access systems.

Mr. Miki is a member of the IEICEJ. He received the IEICEJ Achievement Award in 1999.

Kiyomi Kumozaki (M'02) received the B.E. and M.E. degrees in electrical and electronics engineering from Toyohashi University of Technology, Toyohashi, Japan, in 1980 and 1982, respectively, and the Ph.D degree from Tohoku University, Sendai, Japan, in 2000.

In 1982, He joined the NTT Yokosuka Electrical Communication Laboratory, Kanagawa, Japan, where he was engaged in research on metallic digital transmission and development of metallic digital access systems. From 1987 to 1990, he worked on the development of ISDN basic rate access systems at the NTT Network Systems Development Center, Kanagawa. From 1991 to 1997, he was with the NTT Transmission Systems Laboratories, Kanagawa, where he carried out research on passive optical access networks for providing data communication, telephony, and video distribution services. From 1998 to 2000, he worked for NTT Communications Corporations, Tokyo, Japan, where he was engaged in building large-scale LAN, WAN, and global network infrastructure for business enterprise. Since 2001, he has been with the NTT Access Service Systems Laboratories and is working on research and development of next-generation access networks including high-speed passive optical networks.

Takamasa Imai received the B.E., M.E., and Dr.Eng. degrees in electronics engineering from Osaka University, Osaka, Japan, in 1980, 1982, and 1992, respectively.

In 1982, he joined the NTT Laboratories, where he has been engaged in the research and development of optical fiber transmission systems including long-distance and access systems. Since 2007, he has been a Professor of the Faculty of Engineering of Kanagawa University, Kanagawa, Japan. He served as a vice-chair of the Paper Committee of SubOptic 2001 in Kyoto.

Dr. Imai received the Young Engineer Award from the IEICEJ in 1990 and IEICEJ Communication Society Activity Testimonial in 2000.

Naoto Yoshimoto (M'94) was born in Hokkaido, Japan, on June 23, 1963. He received the B.S., M.S., and Ph.D. degrees in electronics and information engineering from Hokkaido University, Sapporo, Japan, in 1986, 1988, and 2003, respectively.

In 1988, he joined the NTT Opto-electronics Laboratories, where he was engaged in the research of semiconductor optical devices and their integration technology for constructing future optical fiber communication systems. From 1998 to 2002, he moved to NTT Electronics Corporation, where he was mainly involved with development of high-speed semiconductor laser diode modules and their mass production technology for realizing broadband networks. He is currently the team leader of the Broadband Access Systems Research Group, NTT Access Network Service Systems Laboratories. He has been engaged in the planning and design of next-generation optical access network services and architectures mainly based on WDM-PON and high-speed TDM-PON technologies.

Dr. Yoshimoto is a member of the IEEE Laser Electro-Optical Society and IEICEJ.

Makoto Tsubokawa received the B.S., M.S., and Ph.D. degrees in applied physics from Hokkaido University, Sapporo, Japan in 1981, 1984, and 1989, respectively.

After joining NTT Laboratories in 1984, he has been engaged in research on transmission characteristics of optical fibers, design of optical networks, and access systems. He is currently the Project manager responsible for innovative access system technologies and their portfolio strategy.

Dr. Tsubokawa is a member of the IEICEJ.